

Supplement of Atmos. Chem. Phys., 20, 7979–8001, 2020
<https://doi.org/10.5194/acp-20-7979-2020-supplement>
© Author(s) 2020. This work is distributed under
the Creative Commons Attribution 4.0 License.



Supplement of

Vertical redistribution of moisture and aerosol in orographic mixed-phase clouds

Annette K. Miltenberger et al.

Correspondence to: Annette K. Miltenberger (amiltenb@uni-mainz.de)

The copyright of individual parts of the supplement might differ from the CC BY 4.0 License.

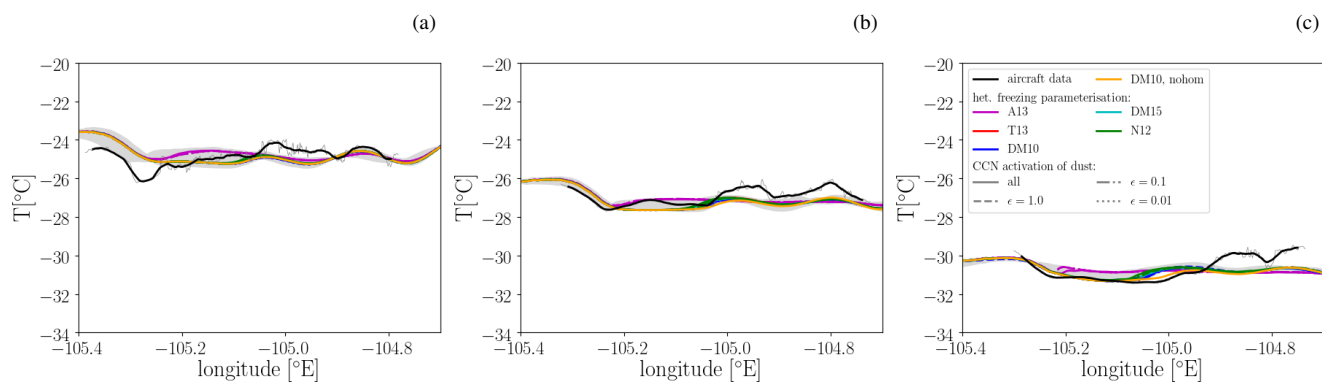


Figure S1. Comparison of air temperature for the three different flight legs. The lowest flight leg is shown in (a) and the highest one in (c). The thick black lines shows the smoothed aircraft data (thin black line shows 1 Hz data). Model data are interpolated to the same tangents of the mean streamlines as used in Fig. 3 of the main paper. The variability of the variables along all these hypothetical flight paths are shown by the grey shading, while the thick coloured lines show the median values for simulations. The different coloured lines represent with different ice nucleation schemes and different line styles indicate different assumptions on the amount of soluble material in the dust particles.

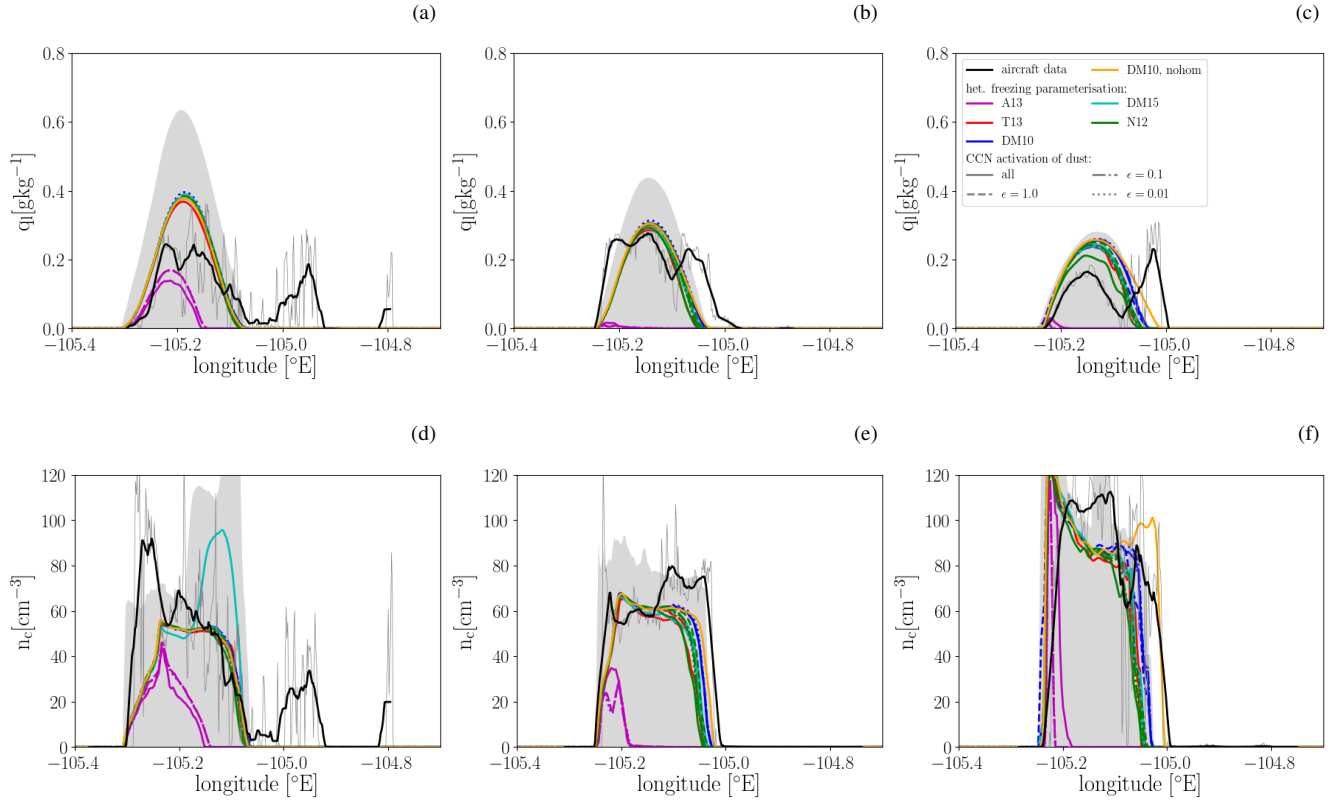


Figure S2. Comparison of (a-c) liquid water content and (d-f) cloud droplet number concentration for the three different flight legs. The lowest flight leg is shown in (a, d) and the highest one in (c, f). The thick black lines shows the smoothed aircraft data (thin black line shows 1 Hz data). Model data are interpolated to the same tangents of the mean streamlines as used in Fig. 3 of the main paper. The variability of the variables along all these hypothetical flight paths are shown by the grey shading, while the thick coloured lines show the median values for simulations. The different coloured lines represent with different ice nucleation schemes and different line styles indicate different assumptions on the amount of soluble material in the dust particles.

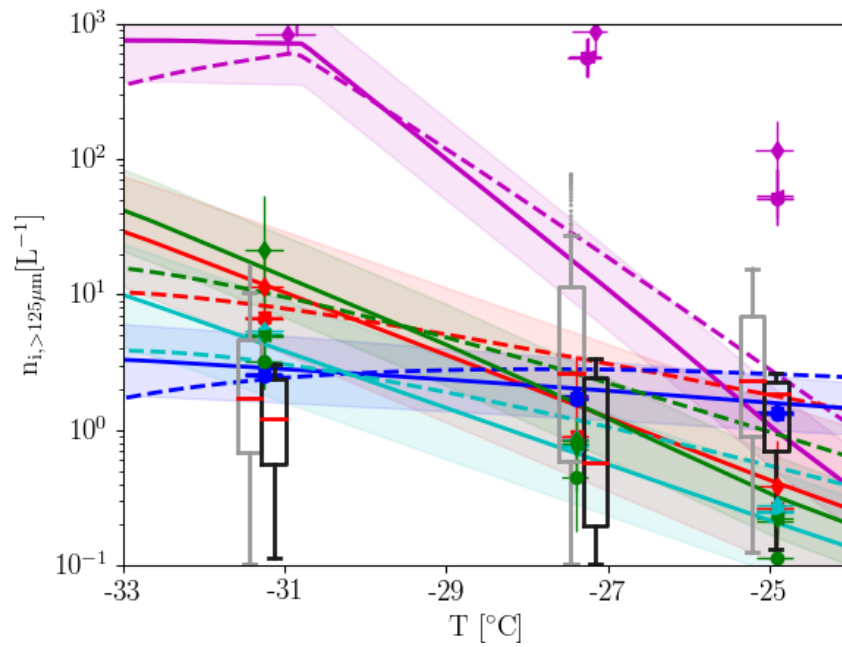


Figure S3. Same as Fig. 6 in the main paper, but assuming feldspar to cover 1 % of the dust surface instead of 1 % in the A13 parameterisation (magenta lines and shading).

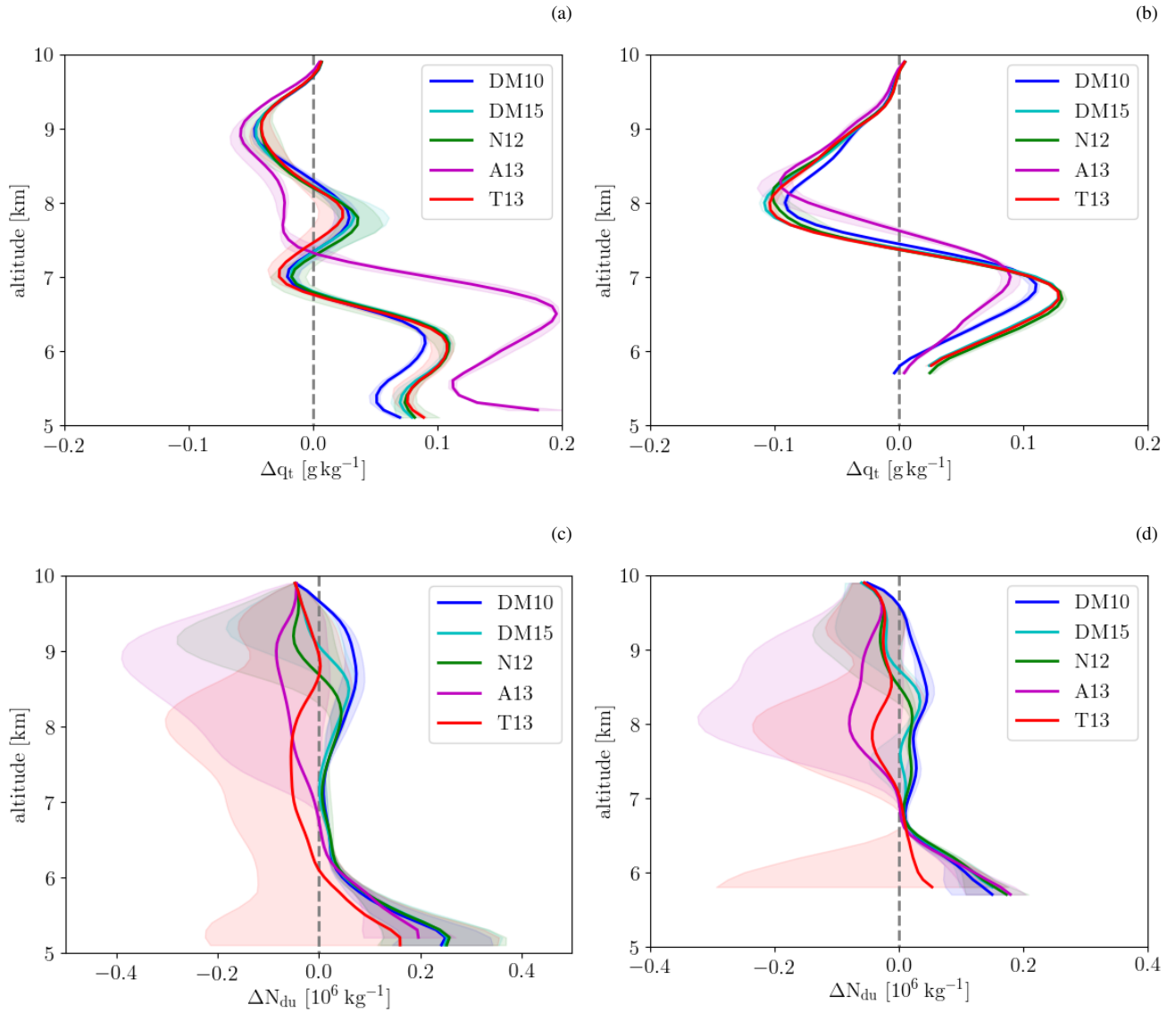


Figure S4. Mean profiles of Δq_t (a, b) and ΔN_{du} (c, d) for all simulations averaged between 2110 – 2130 UTC (a, c) and 2140 – 2200 UTC (b, d). The different colours correspond to simulations with different ice nucleation parameterisations, while the shading represents the variability due different assumptions on the CCN activation of dust.

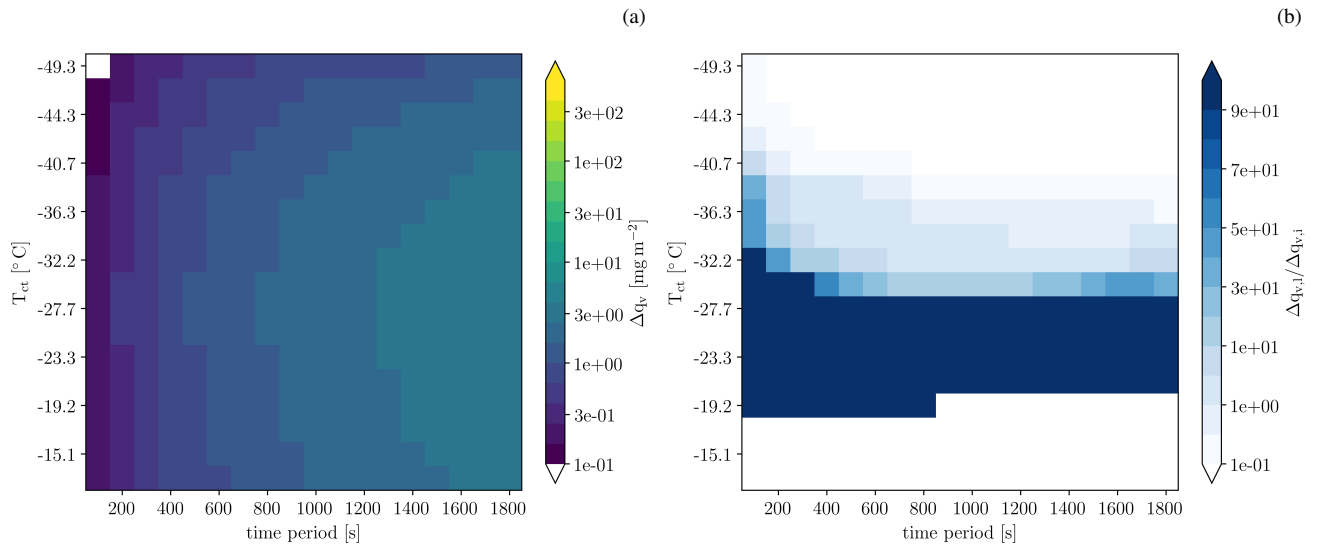


Figure S5. (a) Modification of total water profiles by sedimentation of cloud droplets across wave clouds with vertical extend z_c of 2500 m and various cloud top temperatures (ordinate) as well as periods (abscissa). The mean value across KiD-simulations with different ice nucleation and soluble fraction descriptions is shown. (b) Ratio between the modification of total water profiles by sedimentation of liquid hydrometeor compared to that of frozen hydrometeors. The mean values over the same set of experiments as in (a) are used.

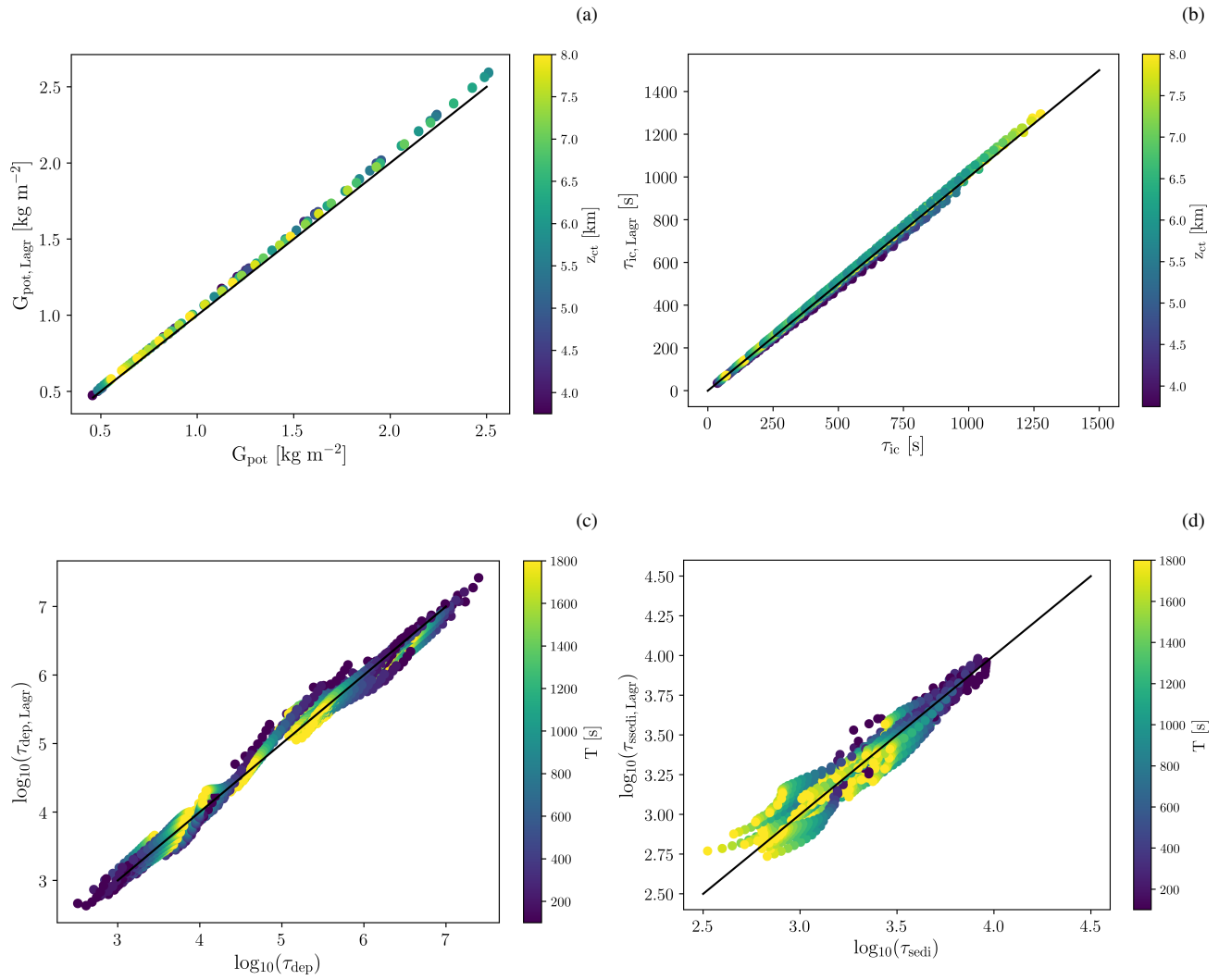


Figure S6. Comparison of Lagrangian estimates (ordinate) and analytical approximations (abscissa) for (a) G_{pot} , (b) τ_{ic} , (c) τ_{dep} , and (d) τ_{sedi} .

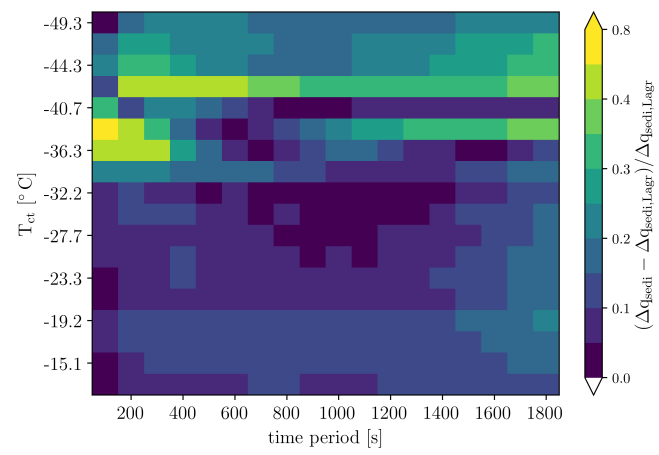


Figure S7. Relative difference between the downward moisture transport computed from the KiD simulations and predicted by the conceptual model. Results are shown for a cloud thickness of 2 km.